A spin-flip variant of the second-order approximate coupled-cluster singles and doubles method

Garrette Pauley Paran,[1] Cansu Utku,[1] and Thomas-Christian Jagau*[1]
Department of Chemistry, KU Leuven, Celestijnenlaan 200F, 3001 Leuven, Belgium

(*Electronic mail: thomas.jagau@kuleuven.be)

(Dated: 11 October 2022)

We report an implementation of a spin-flip variant of the second-order approximate coupled-cluster singles and doubles (CC2) method. The resolution-of-the-identity approximation or, alternatively, Cholesky decomposition of the two-electron integrals are used to reduce the memory requirements. We illustrate the performance of the new method by constructing potential energy curves of H_2 and HF and by computing singlet-triplet splittings for various diradicals including some binuclear copper complexes that are of interest as molecular magnets. We find that spin-flip CC2 performs very similarly to the spin-flip variant of the algebraic diagrammatic construction scheme for the polarization propagator of second order (ADC(2)). Application to ozone shows that spin-flip CC2 predicts a barrierless symmetric dissociation of this molecule similar to spin-conserving CC2 and in contrast to spin-flip ADC(2) and coupled-cluster singles and doubles.

I. INTRODUCTION

Wave functions with multiconfigurational character are ubiquitous in chemistry.[1] Examples of molecules with a multiconfigurational ground state at the equilibrium structure include organic diradicals and transition metal compounds, which feature degenerate or near-degenerate frontier orbitals. Moreover, bond breaking inevitably results in multiconfigurational wave functions. A description of such systems with single-reference methods breaks down because the Hartree-Fock (HF) reference wave function is qualitatively incorrect.

One approach to multiconfigurational wave functions consists in multireference methods. Here, one constructs a multiconfigurational self-consistent field wave function[2,3] for the target state and treats dynamical correlation by means of multireference variants of perturbation theory,[4–7] configuration interaction (CI),[8–11] or coupled-cluster (CC) theory.[12–17] In recent years, the density matrix renormalization group has emerged as a further approach.[18,19]

An alternative to treating multiconfigurational wave functions directly is provided by equation-of-motion, response theory, and propagator methods. Here, one first computes the HF wave function of some reference state that is well approximated by a single Slater determinant, then treats dynamical correlation for this reference state using a single-reference method, and finally constructs the correlated target state from the correlated reference.

A particular variant of this idea is the spin-flip (SF) approach[20–22] where the reference state and the target state have the same number of electrons but differ in the spin quantum number M_S. The SF approach is motivated by the fact that the component of a multiplet with the highest possible M_S value is usually well approximated by a single Slater determinant not only near the equilibrium structure but at stretched bond lengths as well. This is not the case for singlet states and the low-spin components of higher spin states.[21,22] High-spin determinants are thus well suited to serve as reference for the treatment of low-spin target states with multiconfigurational character by means of spin-flipping excitations. This is illustrated in Fig. 1. Most often, problematic singlet states are treated based on a triplet reference but treatments of doublets based on quartet reference states have been reported as well.[22] Originally introduced in the framework of equation-of-motion (EOM) CC theory,[21,23–26] SF variants of many further methods have been established by now. This includes CI[27–32] and algebraic diagrammatic construction methods[33,34] as well as density functional theory.[35–39] In addition, double SF methods,[40] which can describe singlet states based on a high-spin quintet reference, as well as approaches that allow for an arbitrary number of spin flips[41] have been introduced. Numerous applications to bond breaking,[42] to organic diradicals, triradicals, and polyradicals,[43–52] to conical intersections,[53–57] to non-adiabatic excited-state dynamics,[58–60], to dipole polarizabilities[61,62] and to magnetic properties of transition metal compounds,[63–68] demonstrate that SF methods constitute a viable alternative to the more traditional multireference approaches.

In this work, we report an SF variant of the second-order approximate coupled-cluster singles and doubles (CC2) method.[69] CC2 has been developed in the context of CC linear response theory (LRT),[70–73] which is closely related to EOM-CC theory.[74–77] The method arises from a perturbative analysis of the CC singles and doubles (CCSD) equations in terms of the fluctuation potential. The one-particle part of the normal-ordered Hamiltonian (F) and the single amplitudes (T_1) are assigned to be zeroth order, whereas the two-particle part of the normal-ordered Hamiltonian, i.e., the fluctuation potential W, and the double amplitudes T_2 are assigned to be first order. One then retains only first-order and zeroth-order terms in the doubles amplitude equations, while the singles amplitude equations are not modified. This results in[69]

$$\Omega_i^a = \langle \Phi_i^a | e^{-T_1} H e^{T_1} + [e^{-T_1} H e^{T_1}, T_2] | \Phi_0 \rangle = 0 \,, \quad (1)$$

$$\Omega_{ij}^{ab} = \langle \Phi_{ij}^{ab} | e^{-T_1} H e^{T_1} + [F, T_2] | \Phi_0 \rangle = 0 \,. \quad (2)$$

Since CC-LRT can be applied to the CC2 model in the same way as to CCSD, it is possible to derive response functions and to define excitation energies for CC2 wave functions as eigenvalues of a Jacobian.[69,73]

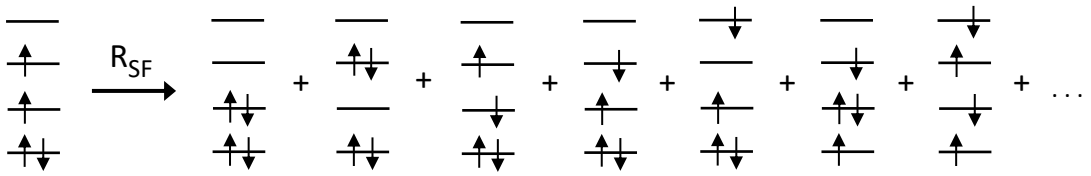

FIG. 1. Description of a low-spin state as spin-flipping excitation from a high-spin reference state.

CC2 is well established as a method for excited states[69,78–89] that can be applied to much larger systems than EOM-CCSD because the computational cost scales less steeply (N^5 as compared to N^6, where N is the system size). Commonly, CC2 is combined with the resolution-of-the-identity (RI) approximation[79] or Cholesky decomposition[83] of the electron repulsion integrals (ERIs). This is advantageous because the memory requirements can be reduced from N^4 to N^3 if one rewrites the amplitude equations in terms of $e^{-T_1}He^{T_1}$, i.e., a Hamiltonian that is similarity-transformed by T_1. The double amplitude equations then assume a form similar to second-order Møller-Plesset perturbation theory (MP2) so that T_2 can be computed on the fly and does not need to be stored.

We note that CC2 is closely related to algebraic diagrammatic construction through second order (ADC(2));[33,34,90–93] the two methods often yields very similar results. Starting from the CC2 Jacobian derived within CC-LRT, one can obtain the ADC(2) secular matrix by setting to zero the singles amplitudes (T_1) and replacing the CC2 T_2 amplitudes by those from MP2 followed by symmetrization of the Jacobian.[84] Another closely related method is CIS(D),[94,95] for which a spin-flip variant has been introduced as well.[28]

The SF-CC2 implementation reported in the present work is suitable for unrestricted (UHF) and restricted open-shell (ROHF) reference wave functions. The RI approximation or, alternatively, Cholesky decomposition, can be applied to the ERIs. However, our implementation is not based on a T_1-transformed Hamiltonian; rather it relies on modified CCSD and EOM-CCSD equations. The working equations of SF-CC2 and standard CC2 are the same in a spin-orbital formulation and differ only in the spin symmetry of the excitation amplitudes. This is the same for spin-flipping and spin-conserving EOM-CCSD.[23] The details of the computations that we performed to illustrate the performance of SF-CC2 are provided in Section II. The corresponding results are presented in Section III and compared to CCSD and ADC(2) results, while Section IV summarizes our general conclusions.

II. COMPUTATIONAL DETAILS

We have implemented the SF-CC2 method into the Q-CHEM electronic-structure package[96] making use of the libtensor library.[97] To assess its performance, we studied the following cases:

- Potential energy curves of the ground states of the hydrogen molecule (H_2) and the hydrogen fluoride molecule (HF).

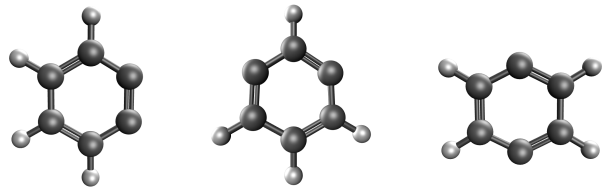

FIG. 2. Structures of *ortho*-benzyne (left), *meta*-benzyne (middle), and *para*-benzyne (right).

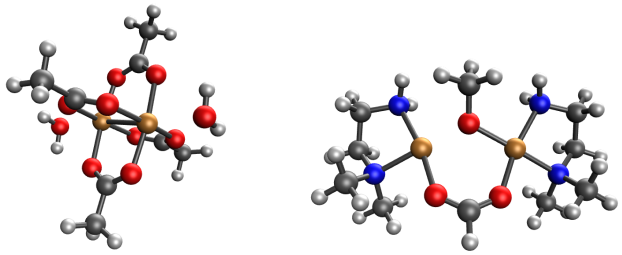

FIG. 3. Structures of the binuclear copper complexes $Cu_2(CH_3COO)_4(H_2O)_2$ (CUAQAC02, left) and $[Cu_2(C_4H_{12}N_2)_2(OCH_3)(O_2CH)]^{2+}$ (PATFIA without ferrocene ligand, right).

- Vertical singlet-triplet splittings between the $^1\Delta$ and $^3\Sigma^-$ states of NH, OH^+, and NF and between the $^1\Delta_g$ and $^3\Sigma_g^-$ states of O_2. The wave functions of the Δ states are dominated by two exactly degenerate determinants. The bond lengths used are R(NH) = 1.036 Å, R(NF) = 1.317 Å, R(OH) = 1.029 Å, R(OO) = 1.207 Å.

- Vertical singlet-triplet splittings between the $^1A_1$ and $^3B_1$ states of CH_2, NH_2^+, SiH_2, and PH_2^+. The wave functions of the $^1A_1$ states all have only moderate multiconfigurational character, but the singlet-triplet splittings vary significantly. The bond lengths and angles used are R(CH) = 1.0775 Å, R(NH) = 1.0295 Å, R(SiH) = 1.4770 Å, R(PH) = 1.4056 Å and ∠(HCH) = 133.29°, ∠(HNH) = 150.88°, ∠(HSiH) = 118.26°, and ∠(HPH) = 121.77°.

- Vertical singlet-triplet splittings of *ortho*-, *meta*-, and *para*-benzyne. The multiconfigurational character of the singlet state grows in the order *ortho* < *meta* < *para*, the singlet-triplet splittings decrease in the same order. The molecular structures (Fig. 2), optimized for the triplet states, were taken from Ref. 43 and are available in the electronic supplementary information (ESI).

- Vertical singlet-triplet splittings of two

binuclear copper complexes: tetra-μ-acetato-bisaquo-dicopper(II) (CUAQAC02), $Cu_2(CH_3COO)_4(H_2O)_2$ and μ-methoxo-μ-formiato-tetra-(N,N-dimethylethylenediamine)-dicopper(II) (PATFIA without ferrocene ligand), $[Cu_2(C_4H_{12}N_2)_2(OCH_3)(O_2CH)]^{2+}$. The molecular structures of these complexes (Fig. 3) were taken from Refs. 68 and 67, respectively, and are available in the ESI.

- Potential energy curves of the ground state of ozone (O_3) at an O-O-O angle of 142.76°. This investigation is motivated by the failure of CC2 reported in Ref. 98. A second set of calculations carried out at the equilibrium bond angle (116.78°) is reported in the ESI (Fig. 1).

In all calculations, the cc-pVXZ (X = D, T, Q) basis sets[99,100] were employed if not stated otherwise. Core electrons were frozen in the correlation treatment of the copper complexes and included for all other calculations. The corresponding auxiliary basis sets[101] were employed for calculations using the RI approximation. A threshold of 10^{-3} was used in all cases where Cholesky decomposition of the ERIs was applied. All SF-CC2 results are compared to results from EOM-SF-CCSD and SF-ADC(2) calculations that were carried out with Q-CHEM as well.

For the calculation of the singlet-triplet splittings of the diatomics, the carbene-like molecules, and the three isomers of benzyne, we used UHF and ROHF references while the potential curves of H_2, HF, and O_3 as well as the singlet triplet splittings of the two copper complexes were computed only with UHF. We note that, although the spin contamination of ROHF-CC wave functions is usually smaller than that of UHF-CC wave functions, it can hardly be said that ROHF-CC is generally superior.

We use the $M_S = 0$ component of the triplet state, which is obtained as spin-flipping excitation with all methods, for the evaluation of singlet-triplet splittings. It has been argued in the context of EOM-SF-CCSD that this provides a more balanced description than using the reference state ($M_S = 1$).[77] We define the splitting as $E_{\text{singlet}} - E_{\text{triplet}}$ meaning that positive values correspond to a triplet ground state.

III. RESULTS AND DISCUSSION

A. Potential energy curves of H_2 and HF

As a first numerical test of the SF-CC2 method, we computed potential energy curves for the $^1\Sigma_g^+$ and $^1\Sigma^+$ ground states of H_2 and HF, which are shown in Fig. 4. For both molecules, we also performed SF-ADC(2) and EOM-SF-CCSD calculations that are reported in Fig. 4 as well. These calculations all use the $^3\Sigma_u^+$ state of H_2 and the $^3\Sigma^+$ state of HF as reference. For HF, we compare to the full CI values from Ref. 102, whereas for a two-electron system such as H_2, EOM-SF-CCSD yields the same energies as full CI so that this curve serves as reference.

The upper panels of Fig. 4 demonstrate that all SF methods yield qualitatively correct potential energy curves for both molecules, while it is well known that a direct treatment of the ground state with truncated methods does not describe the dissociation correctly. A more thorough analysis is possible based on the lower panels of Fig. 4 that present the same results as deviations from full CI. For H_2, the SF-CC2 and SF-ADC(2) curves lie practically on top of each other with deviations not exceeding 10^{-4} a.u. Both methods underestimate the dissociation energy by ca. 0.009 a.u. (0.25 eV) while the agreement with full CI is better near the equilibrium bond length.

For HF, more substantial differences between SF-CC2 and SF-ADC(2) are visible. SF-ADC(2) underestimates the dissociation energy by ca. 0.016 a.u. (0.44 eV) while the corresponding value for SF-CC2 amounts to 0.009 a.u. (0.25 eV). As can be expected, EOM-SF-CCSD is clearly superior underestimating the dissociation energy by less than 10^{-4} a.u. (0.0025 eV). The most significant discrepancies with full CI occur for all methods at intermediate distances. SF-CC2 yields a maximum deviation of 0.023 a.u. (0.62 eV) at 1.6 Å, the corresponding value for SF-ADC(2) amounts to 0.020 a.u. (0.55 eV) at 1.4 Å. EOM-SF-CCSD performs somewhat better yielding a maximum deviation of 0.011 a.u. (0.31 eV) at 1.8 Å.

The resulting nonparallelity errors (NPEs) for the HF potential energy curve are 0.011 a.u. for EOM-SF-CCSD, 0.032 a.u. for SF-CC2, and 0.037 a.u. for SF-ADC(2). Notably, these values, including the one for EOM-SF-CCSD, are all relatively high compared to multireference methods that take account of dynamic correlation. For example, multireference CI with an active space of two orbitals produces in the DZV basis an NPE of less than 0.001 a.u. for the HF potential energy curve,[103] for state-specific multireference CCSD the value is less than 0.002 a.u.,[103] and internally-contracted multireference CCSD even has an NPE of just 10^{-4} a.u.[14] Multireference variants of second-order perturbation theory in the cc-pVDZ basis also yield NPEs below 0.007 a.u.[104]

B. Singlet-triplet splittings

To investigate the performance of SF-CC2 further, we computed vertical singlet-triplet splittings of various molecules. Tab. I shows the results for the diatomic molecules NH, OH^+, O_2, and NF, all of which have a triplet ground state with the nominal configuration $(\pi_x)^1(\pi_y)^1$ and an excited $^1\Delta$ state with the electronic structure $(\pi_x)^2 + (\pi_y)^2$ where two determinants contribute equally. All spin-flip methods preserve this degeneracy and Tab. I illustrates that the second-order methods SF-CC2 and SF-ADC(2) reproduce the EOM-SF-CCSD results very well. The mean absolute errors (MAEs) relative to EOM-SF-CCSD are 0.021 eV for SF-CC2 and 0.016 eV for SF-ADC(2) with negligible differences between UHF and ROHF variants. The maximum errors amount to 0.051 eV for SF-CC2 and 0.043 eV for SF-ADC(2). We note that the error introduced by the RI approximation is of the order of 10^{-4} eV and thus much smaller except for the cc-pVDZ basis set.

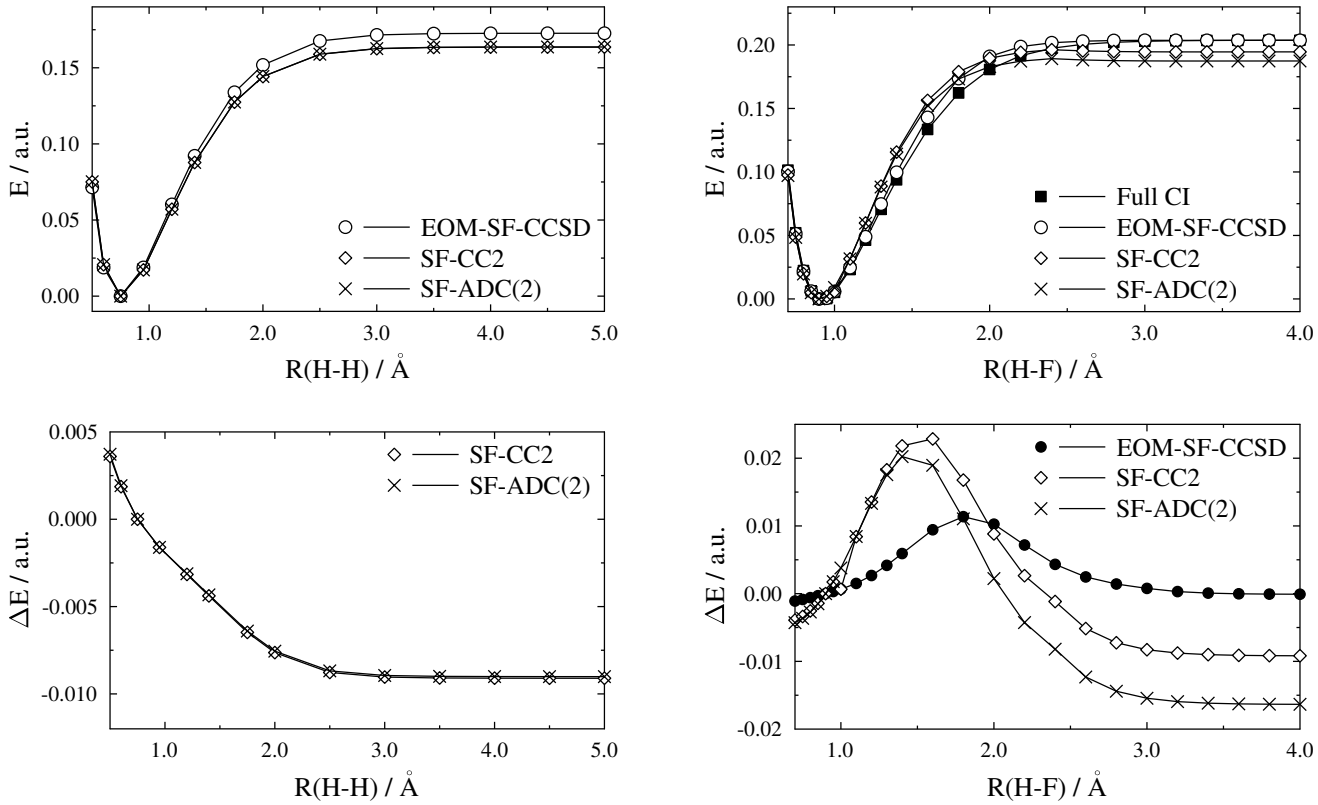

FIG. 4. Upper panels: Potential energy curves for the ground states of H_2 (left) and HF (right) computed with EOM-SF-CCSD, SF-CC2, and SF-ADC(2). For HF, full CI results from Ref. 102 are shown as well. The energy at the equilibrium structure is set to zero for all curves. The cc-pVTZ basis set is used for H_2, the 6-31G** basis set for HF. Lower panels: The same data plotted as deviations from full CI.

TABLE I. Vertical singlet-triplet gaps in eV of NH, OH^+, O_2, and NF computed at the equilibrium structures of the triplet states.

		UHF				ROHF			
	Basis	EOM-SF-CCSD	SF-CC2	SF-RI-CC2	SF-ADC(2)	EOM-SF-CCSD	SF-CC2	SF-RI-CC2	SF-ADC(2)
NH	cc-pVDZ	1.8216	1.8003	1.8005	1.8060	1.8214	1.8006	1.8006	1.7944
	cc-pVTZ	1.6590	1.6555	1.6555	1.6642	1.6581	1.6555	1.6555	1.6543
	cc-pVQZ	1.6064	1.6042	1.6043	1.6142	1.6051	1.6040	1.6041	1.6046
OH^+	cc-pVDZ	2.3653	2.3296	2.3293	2.3353	2.3654	2.3298	2.3294	2.3223
	cc-pVTZ	2.2363	2.2173	2.2174	2.2243	2.2360	2.2181	2.2182	2.2137
	cc-pVQZ	2.1888	2.1722	2.1723	2.1794	2.1883	2.1731	2.1732	2.1697
O_2	cc-pVDZ	1.1127	1.1401	1.1361	1.1511	1.1088	1.1361	1.1320	1.1342
	cc-pVTZ	1.0715	1.0794	1.0794	1.0936	1.0667	1.0746	1.0745	1.0738
	cc-pVQZ	1.0542	1.0541	1.0542	1.0695	1.0488	1.0486	1.0487	1.0481
NF	cc-pVDZ	1.6520	1.6023	1.6005	1.6352	1.6518	1.6026	1.6009	1.6205
	cc-pVTZ	1.5389	1.5012	1.5010	1.5353	1.5383	1.5021	1.5019	1.5226
	cc-pVQZ	1.5033	1.4653	1.4654	1.4995	1.5025	1.4662	1.4664	1.4871

However, the good performance of SF-CC2 and SF-ADC(2) apparent from Tab. I should be treated with care. In the ESI (Tab. 2), we report energy differences between the reference states ($M_S = 1$) and the $M_S = 0$ components of the same triplet states. Since this multiplet splitting vanishes in the exact limit, its value provides a measure for the quality of an approximate wave function. For EOM-SF-CCSD with UHF and ROHF references, we obtain values of 0.01–0.03 eV and <0.0001 eV, respectively, whereas SF-CC2 yields 0.13–0.26 eV starting from a UHF reference and 0.05–0.19 eV starting from an ROHF reference. For SF-ADC(2) compared to the MP2 reference state, the artificial multiplet splitting is even more pronounced with values of up to 0.39 eV for UHF-based calculations and up to 0.30 eV for ROHF-based calculations. Interestingly, the $M_S = 0$ state computed with ROHF-SF-ADC(2) has a lower energy than the ROHF-MP2 reference state whereas the $M_S = 0$ state is higher in energy in all other cases. This outlier can probably be related to the poor general performance of ROHF-MP2.[1] In conclusion, our results demonstrate that the suggestion from Ref. 77 to evaluate singlet-triplet splittings

TABLE II. Vertical singlet-triplet gaps in eV of CH_2, NH_2^+, SiH_2, and PH_2^+ computed at the equilibrium structures of the triplet states.

		UHF				ROHF			
	Basis	EOM-SF-CCSD	SF-CC2	SF-RI-CC2	SF-ADC(2)	EOM-SF-CCSD	SF-CC2	SF-RI-CC2	SF-ADC(2)
CH_2	cc-pVDZ	1.0780	1.1441	1.1444	1.1492	1.0766	1.1452	1.1455	1.1432
	cc-pVTZ	0.9403	1.0129	1.0130	1.0233	0.9384	1.0150	1.0151	1.0206
	cc-pVQZ	0.9022	0.9675	0.9676	0.9800	0.9001	0.9700	0.9700	0.9784
NH_2^+	cc-pVDZ	1.9597	1.9537	1.9537	1.9613	1.9592	1.9524	1.9524	1.9417
	cc-pVTZ	1.8220	1.8273	1.8273	1.8381	1.8208	1.8272	1.8272	1.8224
	cc-pVQZ	1.7804	1.7824	1.7825	1.7941	1.7790	1.7827	1.7829	1.7797
SiH_2	cc-pVDZ	-0.3520	-0.2438	-0.2446	-0.2484	-0.3534	-0.2421	-0.2430	-0.2478
	cc-pVTZ	-0.4333	-0.3399	-0.3399	-0.3451	-0.4347	-0.3378	-0.3379	-0.3441
	cc-pVQZ	-0.4572	-0.3769	-0.3768	-0.3823	-0.4586	-0.3747	-0.3747	-0.3810
PH_2^+	cc-pVDZ	-0.0947	-0.0070	0.0066	-0.0042	-0.0964	0.0090	0.0085	-0.0038
	cc-pVTZ	-0.1886	-0.0948	-0.0945	-0.0970	-0.1904	-0.0922	-0.0920	-0.0966
	cc-pVQZ	-0.2161	-0.1342	-0.1340	-0.1360	-0.2179	-0.1315	-0.1314	-0.1353

using the $M_S = 0$ component of the triplet state is vital for SF-CC2 and SF-ADC(2), whereas it only represents a marginal improvement in the case of EOM-SF-CCSD.

As a second set of test cases, we studied CH_2, NH_2^+, SiH_2 and PH_2^+ all of which have frontier orbitals of a_1 and b_1 symmetry. Both orbitals are formally nonbonding but the a_1 orbital is located in the molecular plane, whereas the b_1 orbital is oriented perpendicular to the molecular plane. In the $^3B_1$ states, both orbitals are singly occupied, while the $^1A_1$ states are dominated by the determinant where the a_1 orbital is doubly occupied. However, the determinant where the b_1 orbital is doubly occupied delivers a significant contribution as well.

In the ESI (Tab. 3), we report the leading amplitudes from SF-CC2, SF-ADC(2), and EOM-SF-CCSD calculations, which illustrates that all methods agree on the moderate multiconfigurational character of the $^1A_1$ states. According to our calculations it grows in the order $PH_2^+ < SiH_2 < CH_2 < NH_2^+$; for the first molecule the two most important determinants have coefficients of 0.94 and 0.17, for the last molecule the values are 0.81 and 0.47.

It is well established that CH_2 and NH_2^+ have a triplet ground state while SiH_2 and PH_2^+ have a singlet ground state.[43] Our computed singlet-triplet splittings in Tab. II reproduce that. SF-CC2 and SF-ADC(2) perform very similarly to each other and at the same time somewhat worse than for the diatomics. The MAEs relative to EOM-SF-CCSD amount to 0.065 eV for SF-CC2 and 0.066 eV for SF-ADC(2), the maximum errors are 0.111 eV and 0.106 eV, respectively. Notably, SF-CC2 yields the wrong sign for the singlet-triplet gap of PH_2^+ if the cc-pVDZ basis is employed; the deviation from EOM-SF-CCSD is of the same size as the actual singlet-triplet gap. We note that the trends in the multiplet splittings are similar to those observed for the diatomic molecules and that differences between UHF and ROHF-based calculations are again negligible.

Next, we applied SF-CC2 to compute singlet-triplet splittings for the three isomers of benzyne. These molecules served as test cases for other SF methods in the past[25,43] and we note that these previous studies focused on the adiabatic energy gap, which has been determined experimentally.[105] However, since the purpose of the present work is to assess the SF-CC2 method, we limit ourselves to vertical energy splittings in the following.

The electronic structure of the benzyne molecules is governed by two frontier orbitals that can be understood as bonding and antibonding combinations of the orbitals hosting the two unpaired electrons.[106] Because the energy gap between these two orbitals decreases from *ortho*-benzyne over *meta*-benzyne to *para*-benzyne, the multiconfigurational character of the singlet state grows in the same order. This trend is apparent in the two leading amplitudes of all SF calculations, which assume values of 0.83 and 0.21 for *ortho*-benzyne, of 0.77 and 0.28 for *meta*-benzyne and of 0.66 and 0.50 for *para*-benzyne (see ESI, Tab. 3).

It is well known that all isomers of benzyne have a singlet ground state[105,106] although the singlet-triplet gap shrinks considerably in the order *ortho* > *meta* > *para*.[106] Our computed singlet-triplet splittings in Tab. III conform to this trend. Here, the differences between SF-CC2 and SF-ADC(2) are a little more pronounced than in Tabs. I and II: The MAE relative to EOM-SF-CCSD amounts to 0.031 eV for SF-CC2 as compared to 0.021 eV for SF-ADC(2) and the maximum errors are 0.076 eV for SF-CC2 and 0.065 eV for SF-ADC(2). Tab. III shows that all second-order methods except UHF-SF-ADC(2) perform noticeably worse for *m*-benzyne than for the other two isomers. Whereas the substantial spin contamination of the UHF reference determinant ($\langle S^2 \rangle \approx 2.68$) suggests than ROHF might give better results for *m*-benzyne, Tab. III shows that this is not the case: The deviations from EOM-SF-CCSD are in fact larger than with the UHF-based methods.

Using the $M_S = 0$ component of the triplet state for the evaluation of the singlet-triplet splitting is again indispensable for all SF-CC2 and SF-ADC(2) calculations because of the large multiplet splittings (see ESI, Tab. 2). This artificial splitting is especially pronounced for *m*-benzyne with values of 0.17 eV, 0.34 eV, and 0.42 eV for EOM-SF-CCSD, SF-CC2, and SF-ADC(2), respectively.

To illustrate the applicability of SF-CC2 to somewhat larger molecules, we computed singlet-triplet splittings for two binuclear copper complexes, $Cu_2(CH_3COO)_4(H_2O)_2$ (CUAQAC02) and $[Cu_2(C_4H_{12}N_2)_2(OCH_3)(O_2CH)]^{2+}$ (PATFIA without ferrocene group) using the cc-pVDZ basis. In the

TABLE III. Vertical singlet-triplet gaps in eV of *ortho*-, *meta*-, and *para*- benzyne computed at the equilibrium structures of the triplet states.

		UHF				ROHF			
	Basis	EOM-SF-CCSD	SF-CC2	SF-RI-CC2	SF-ADC(2)	EOM-SF-CCSD	SF-CC2	SF-RI-CC2	SF-ADC(2)
o-C_6H_4[a]	cc-pVDZ	-1.0397	-1.0338	-1.0348	-1.0068	-1.0435	-1.0395	-1.0405	-1.0123
	cc-pVTZ	-1.0305	-1.0467	-1.0468	-1.0181	-1.0343	-1.0529	-1.0531	-1.0237
	cc-pVQZ	-1.0362	-1.0605	-1.0605	-1.0325	-1.0401	-1.0669	-1.0670	-1.0384
m-C_6H_4[a]	cc-pVDZ	-0.5032	-0.5438	-0.5442	-0.5175	-0.5128	-0.5797	-0.5802	-0.5735
	cc-pVTZ	-0.5082	-0.5552	-0.5554	-0.5260	-0.5176	-0.5899	-0.5901	-0.5804
	cc-pVQZ	-0.5075	-0.5585	-0.5585	-0.5281	-0.5166	-0.5927	-0.5927	-0.5818
p-C_6H_4[b]	cc-pVDZ	-0.1541	-0.1634	-0.1638	-0.1406	-0.1551	-0.1641	-0.1645	-0.1384
	cc-pVTZ	-0.1384	-0.1578	-0.1579	-0.1333	-0.1394	-0.1588	-0.1589	-0.1310
	cc-pVQZ	-0.1354	-0.1585	-0.1585	-0.1332	-0.1363	-0.1596	-0.1596	-0.1310

[a] The molecule has C_{2v} symmetry, the relevant electronic states are $^1A_1$ and $^3B_2$.
[b] The molecule has D_{2h} symmetry, the relevant electronic states are ^1A_g and $^3B_{3u}$.

case of CUAQAC02, the calculation comprises 202 electrons and 418 basis functions, in the case of PATFIA 196 electrons and 464 basis functions.

Both molecules are of interest as prototypical single-molecule magnets.[109,110] The two copper atoms in CUAQAC02 and PATFIA are 2.60 Å and 3.46 Å apart, respectively; the coupling between the unpaired electrons, which reside in d-orbitals at the two copper atoms, is very weak leading to a small singlet-triplet splitting. In binuclear metal complexes, the singlet-triplet gap equals the exchange-coupling constant J between the two radical centers, which enters phenomenological spin Hamiltonians for the description of the behavior in a magnetic field.[110] Most importantly, the sign of J determines whether a molecule shows ferromagnetic ($J > 0$) or antiferromagnetic ($J < 0$) behavior. Experimentally, J can be determined from measurements of the magnetic susceptibility.[109,110]

Our computed singlet-triplet splittings for CUAQAC02 and PATFIA are reported in Tab. IV. In agreement with previous EOM-SF-CCSD calculations[68] and the experimental results,[107,108] SF-CC2 and SF-ADC(2) yield for both molecules tiny splittings of less than 1 kcal/mol (= 350 cm^{-1}) with the singlet states as ground states. For PATFIA all methods overestimate the experimental value for the splitting, while for CUAQAC02 the experimental value lies between the theoretical ones. Although Tab. IV illustrates good performance of SF-CC2 and SF-ADC(2), these results should be treated with care given that the MAE of both methods relative to EOM-SF-CCSD (see Tabs. I–III) is of the same order of magnitude as the singlet-triplet splitting of the two complexes.

TABLE IV. Vertical singlet-triplet gaps in cm^{-1} of $Cu_2(CH_3COO)_4(H_2O)_2$ (CUAQAC02) and $[Cu_2(C_4H_{12}N_2)_2(OCH_3)(O_2CH)]^{2+}$ (PATFIA without ferrocene) computed with different spin-flip methods. Experimental values are given as well.

	EOM-SF-CCSD[a]	SF-CC2[b]	SF-ADC(2)[b]	expt
CUAQAC02	-191	-337	-155	-286[c]
PATFIA	-85	-136	-113	-11[d]

[a] From Ref. 68, computed using the cc-pVDZ basis set, Cholesky decomposition (CD) of the ERIs, frozen natural orbitals, and a truncated orbital virtual space.
[b] This work, computed using the cc-pVDZ basis set and CD of the ERIs.
[c] From Ref. 107
[d] From Ref. 108

C. Potential energy surface of ozone

As a final application of SF-CC2, we study the ground electronic state of ozone. Some years ago, it was shown that the standard CC2 method predicts a barrierless symmetric dissociation of that molecule into three oxygen atoms, whereas MP2 and CCSD do not suffer from this failure.[98] The contribution of $[[H,T_1],T_1]$ to the double amplitude equations was identified as a main origin of the problem of CC2 and a connection to the multiconfigurational character of ozone was drawn. Later on, it was shown that internally contracted multireference CC2 has no problem describing the ground state of ozone.[89] The nominal electronic configuration of this state is $(\text{core})^2(4b_2)^2(6a_1)^2(1a_2)^2$ but the configuration $(\text{core})^2(4b_2)^2(6a_1)^2(2b_1)^2$ delivers a non-negligible contribution to the wave function as well.

We constructed PECs for ozone using SF-CC2 and the cc-pVDZ basis set to investigate if the spin-flip variant suffers from the same problem as regular CC2. In addition, we performed EOM-SF-CCSD and SF-ADC(2) calculations. The following four UHF reference wave functions were employed:

- $(\text{core})^2(4b_2)^2(6a_1)^1(1a_2)^2(7a_1)^1$, which corresponds to a $^3A_1$ state;
- $(\text{core})^2(4b_2)^2(6a_1)^1(1a_2)^2(2b_1)^1$, which corresponds to a $^3B_1$ state;
- $(\text{core})^2(4b_2)^2(6a_1)^2(1a_2)^1(2b_1)^1$, which corresponds to a $^3B_2$ state;
- $(\text{core})^2(4b_2)^1(6a_1)^2(1a_2)^2(2b_1)^1$, which corresponds to a $^3A_2$ state;

As is apparent from Fig. 5, the $6a_1$ and $7a_1$ orbitals are σ-type orbitals that are bonding and antibonding along the O-O bonds, respectively. Using the $^3A_1$ state as reference for the

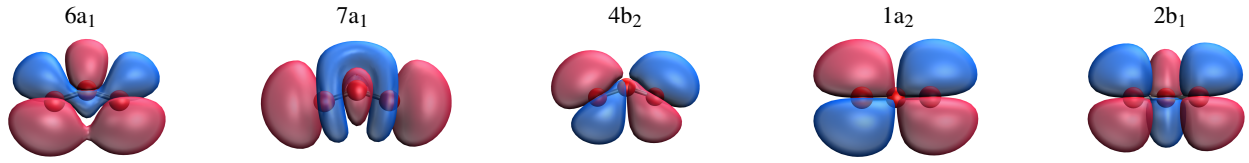

FIG. 5. Relevant molecular orbitals of ozone computed for the $^1A_1$ ground state with the cc-pVDZ basis set at R = 1.30 Å and a bond angle of 142.76° and plotted at an isovalue of 0.02. From left to right: $6a_1$ ($\varepsilon = -0.512$ a.u.), $7a_1$ ($\varepsilon = +0.192$ a.u.), $4b_2$ ($\varepsilon = -0.589$ a.u.), $1a_2$ ($\varepsilon = -0.495$ a.u.), and $2b_1$ ($\varepsilon = -0.044$ a.u.).

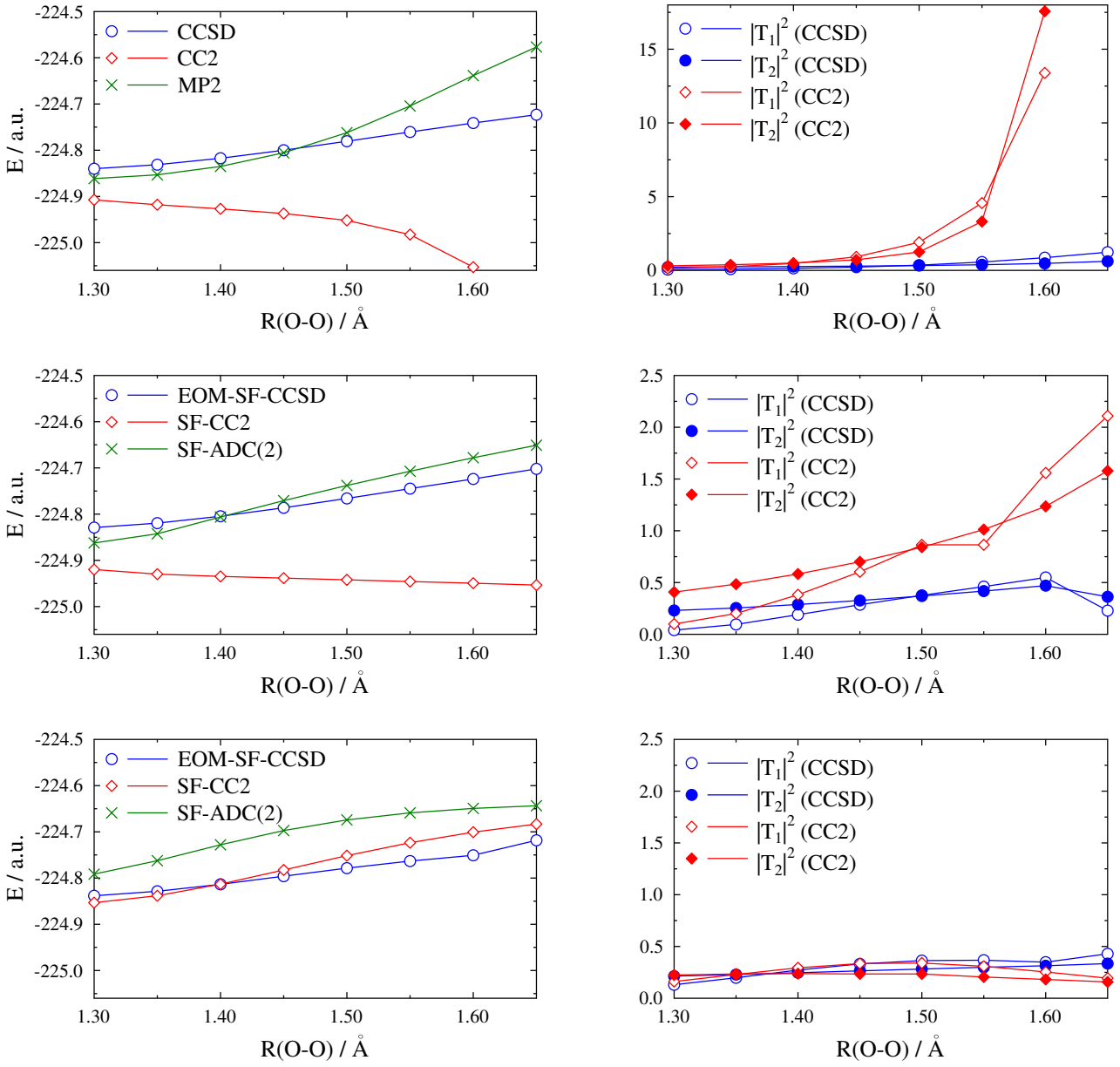

FIG. 6. Left: Potential energy curves of the ground state of ozone at a bond angle of 142.86° computed with conventional CCSD, CC2, and MP2 (top panel), and EOM-SF-CCSD, SF-CC2, and SF-ADC(2) using the $^3A_1$ and $^3A_2$ states as reference (middle and bottom panel). Right: Norms of single and double amplitude vectors from corresponding CCSD and CC2 calculations. The cc-pVDZ basis was used for all calculations.

construction of the PECs is thus best in line with the general idea of SF methods. The other relevant orbitals $4b_2$, $1a_2$, and $2b_1$ have π-character so that the use of the $^3B_1$, $^3B_2$, and $^3A_2$ states as reference is less well justified.

We point out here that, regardless of the choice of reference, all SF methods assume that bond cleavage can be approximated as a two-electrons-in-two-orbitals system, which is questionable in the case of ozone given the non-negligible contributions of two determinants already at the equilibrium structure. As documented in the ESI (Tab. 4), the description of the ground state wave function does not differ much between EOM-SF-CCSD, SF-CC2, and SF-ADC(2) and also not among calculations based on different reference states. At the equilibrium bond length, the two leading amplitudes from the SF calculations are in the ranges 0.916–0.955 and 0.082–0.203, respectively. At stretched bond lengths, the differences are somewhat more pronounced but not striking.

The computed potential energy curves are shown in Fig. 6 together with the norms of the corresponding T_1 and T_2 amplitude vectors. The upper panels reproduce the results from Ref. 98: Whereas CCSD and MP2 yield an increase in energy as the O-O bonds are symmetrically stretched, CC2 yields an erroneous decrease in energy accompanied by a sharp increase in the norms of the CC amplitudes beyond 1.5 Å.

The behavior of SF-CC2 is illustrated in the middle and lower panels of Fig. 6. It is apparent that this depends on the reference state: When the $^3A_1$ state is used, SF-CC2 produces a dissociative curve similar to regular CC2, although with a less steep slope, whereas calculations based on the $^3A_2$ state do not suffer from this failure. SF-CC2 results obtained using the $^3B_1$ and $^3B_2$ states as reference are similar to the ones obtained using the $^3A_2$ state and are reported in the ESI (Fig. 2). The influence of the reference state on the SF-CC2 results is also visible in the CC amplitudes: for the $^3A_1$ state (middle right panel) the norms increase substantially when the O-O bonds are stretched even though this increase is by far not as drastic as for the $^1A_1$ state (upper right panel). In contrast, the norms of the CC amplitude vectors of the $^3A_2$ state (lower right panel) are insensitive towards bond stretching.

We note that SF-ADC(2) produces a qualitatively correct potential energy curve for ozone with all reference states, which is quite remarkable given the very similar performance of SF-CC2 and SF-ADC(2) for all molecules discussed before. At the same time, the different SF-ADC(2) curves deviate more from each other than the EOM-SF-CCSD curves, which is not surprising given the superiority of the latter method. Notwithstanding the failure of SF-CC2 based on the $^3A_1$ state, the qualitative correctness of all other SF curves demonstrates the robustness of the spin-flip approach in view of the multiconfigurational character of the ozone ground state.

IV. CONCLUSIONS

We have presented an implementation of a spin-flip variant of the second-order approximate coupled-cluster singles and doubles model (SF-CC2) together with some representative computations to assess the performance of the method. The spin-flip approach is well established for the treatment of states with multiconfigurational wave functions and is able to describe single-bond breaking correctly. It relies on the fact that high-spin states are often well approximated by a single Slater determinant.

Our implementation of the SF-CC2 method can be combined with the RI approximation or Cholesky decomposition of the ERIs and can handle UHF and ROHF reference determinants. Our calculations illustrate that SF-CC2 delivers results that are very close to those from SF-ADC(2) calculations, which is similar to the behavior of spin-conserving CC2 and ADC(2). The potential energy curve for the ground state of HF shows that SF methods feature substantially larger nonparallelity errors than multireference methods.

For energy differences, the performance is better and SF-CC2 delivers singlet-triplet splittings that typically deviate by 0.02–0.06 eV from EOM-SF-CCSD. However, the use of the low-spin component of the triplet state is vital for evaluating singlet-triplet gaps: The artificial splitting between the low-spin and high-spin components of triplet states is much larger for SF-CC2 (0.05–0.33 eV) and SF-ADC(2) (0.05–0.42 eV) than for EOM-SF-CCSD (< 0.04 eV, often much smaller) owing to the more complete treatment of electron correlation by the latter method.

A noteworthy difference between SF-CC2 and SF-ADC(2) is observed for ozone: SF-CC2 predicts a barrierless symmetric dissociation of that molecule similar to what was observed with conventional CC2. In contrast, SF-ADC(2) yields a qualitatively correct potential energy surface. Interestingly, the failure of SF-CC2 depends on the reference state, it is only present when the $^3A_1$ state is used and can be avoided when using other low-lying triplet states.

In sum, the performance of SF-CC2 is comparable to that of conventional CC2. The reduced accuracy as compared to EOM-SF-CCSD is clearly visible in the numerical results but must be weighed against the reduced computational cost. Given the very similar performance, we imagine for SF-CC2 similar fields of application as for SF-ADC(2).

CONFLICTS OF INTEREST

‘There are no conflicts to declare.

ACKNOWLEDGEMENTS

The authors thank Dr. Pavel Pokhilko for help with the calculations on the copper complexes. T.-C.J. gratefully acknowledges funding from the European Research Council (ERC) under the European Union’s Horizon 2020 research and innovation program (Grant Agreement No. 851766).

[1] A. I. Krylov, *Rev. Comp. Chem.*, 2017, **30**, 151–224.
[2] B. O. Roos, *Adv. Chem. Phys.*, 1987, **69**, 399–445.
[3] R. Shepard, *Adv. Chem. Phys.*, 1987, **69**, 63–200.
[4] K. Andersson, P.-Å. Malmqvist, B. O. Roos, A. J. Sadlej, and K. Wolinski, *J. Phys. Chem.*, 1990, **94**, 5483–5488.

[5]K. Andersson, P.-Å. Malmqvist, and B. O. Roos, *J. Chem. Phys.*, 1992, **96**, 1218–1226.
[6]C. Angeli, R. Cimiraglia, S. Evangelisti, T. Leininger, and J.-P. Malrieu, *J. Chem. Phys.*, 2001, **114**, 10252–10264.
[7]C. Angeli, R. Cimiraglia, and J.-P. Malrieu, *J. Chem. Phys.*, 2002, **117**, 9138–9153.
[8]R. J. Buenker and S. D. Peyerimhoff, *Theor. Chim. Acta.*, 1974, **35**, 33–58.
[9]P. E. M. Siegbahn, *J. Chem. Phys.*, 1980, **72**, 1647–1656.
[10]H.-J. Werner and P. J. Knowles, *J. Chem. Phys.*, 1988, **89**, 5803–5814.
[11]K. R. Shamasundar, G. Knizia, and H.-J. Werner, *J. Chem. Phys.*, 2011, **135**, 054101.
[12]B. Jeziorski and H. J. Monkhorst, *Phys. Rev. A*, 1981, **24**, 1668–1681.
[13]U. S. Mahapatra, B. Datta, and D. Mukherjee, *J. Chem. Phys.*, 1998, **110**, 6171–6188.
[14]F. A. Evangelista, *J. Chem. Phys.*, 2011, **134**, 114102.
[15]M. Hanauer, *J. Chem. Phys.*, 2011, **134**, 204111.
[16]D. I. Lyakh, M. Musiał, V. F. Lotrich, and R. J. Bartlett, *Chem. Rev.*, 2012, **112**, 182–243.
[17]A. Köhn, M. Hanauer, L. A. Mück, T.-C. Jagau, and J. Gauss, *Wiley Interdiscip. Rev.: Comput. Mol. Sci*, 2013, **3**, 176–197.
[18]S. R. White, *Phys. Rev. Lett.*, 1992, **69**, 2863–2866.
[19]A. Baiardi and M. Reiher, *J. Chem. Phys.*, 2020, **152**, 040903.
[20]T.-I. Shibuya and V. McKoy, *Phys. Rev. A*, 1970, **2**, 2208–2218.
[21]A. I. Krylov, *Chem. Phys. Lett.*, 2001, **338**, 375–384.
[22]D. Casanova and A. I. Krylov, *Phys. Chem. Chem. Phys.*, 2020, **22**, 4326–4342.
[23]S. V. Levchenko and A. I. Krylov, *J. Chem. Phys.*, 2004, **120**, 175–185.
[24]L. V. Slipchenko and A. I. Krylov, *J. Chem. Phys.*, 2005, **123**, 084107.
[25]P. U. Manohar and A. I. Krylov, *J. Chem. Phys.*, 2008, **129**, 194105.
[26]A. K. Dutta, S. Pal, and D. Ghosh, *J. Chem. Phys.*, 2013, **139**, 124116.
[27]A. I. Krylov, *Chem. Phys. Lett.*, 2001, **350**, 522–530.
[28]A. I. Krylov and C. D. Sherrill, *J. Chem. Phys.*, 2002, **116**, 3194–3203.
[29]D. Casanova and M. Head-Gordon, *J. Chem. Phys.*, 2008, **129**, 064104.
[30]D. Casanova and M. Head-Gordon, *Phys. Chem. Chem. Phys.*, 2009, **11**, 9779–9790.
[31]N. J. Mayhall, P. R. Horn, E. J. Sundstrom, and M. Head-Gordon, *Phys. Chem. Chem. Phys.*, 2014, **16**, 22694–22705.
[32]J. Mato and M. S. Gordon, *Phys. Chem. Chem. Phys.*, 2018, **20**, 2615–2626.
[33]D. Lefrancois, M. Wormit, and A. Dreuw, *J. Chem. Phys.*, 2015, **143**, 124107.
[34]D. Lefrancois, D. R. Rehn, and A. Dreuw, *J. Chem. Phys.*, 2016, **145**, 084102.
[35]Y. Shao, M. Head-Gordon, and A. I. Krylov, *J. Chem. Phys.*, 2003, **118**, 4807–4818.
[36]F. Wang and T. Ziegler, *J. Chem. Phys.*, 2004, **121**, 12191–12196.
[37]Y. A. Bernard, Y. Shao, and A. I. Krylov, *J. Chem. Phys.*, 2012, **136**, 204103.
[38]X. Zhang and J. M. Herbert, *J. Chem. Phys.*, 2015, **143**, 234107.
[39]M. de Wergifosse, C. Bannwarth, and S. Grimme, *J. Phys. Chem. A*, 2019, **123**, 5815–5825.
[40]D. Casanova, L. V. Slipchenko, A. I. Krylov, and M. Head-Gordon, *J. Chem. Phys.*, 2009, **130**, 044103.
[41]F. Bell, P. M. Zimmerman, D. Casanova, M. Goldey, and M. Head-Gordon, *Phys. Chem. Chem. Phys.*, 2013, **15**, 358–366.
[42]A. A. Golubeva, A. V. Nemukhin, S. J. Klippenstein, L. B. Harding, and A. I. Krylov, *J. Phys. Chem. A*, 2007, **111**, 13264–13271.
[43]L. V. Slipchenko and A. I. Krylov, *J. Chem. Phys.*, 2002, **117**, 4694–4708.
[44]L. V. Slipchenko and A. I. Krylov, *J. Chem. Phys.*, 2003, **118**, 6874–6883.
[45]L. V. Slipchenko, T. E. Munsch, P. G. Wenthold, and A. I. Krylov, *Angew. Chem. Int. Ed.*, 2004, **43**, 742–745.
[46]A.-M. C. Cristian, Y. Shao, and A. I. Krylov, *J. Phys. Chem. A*, 2004, **108**, 6581–6588.
[47]A. I. Krylov, *J. Phys. Chem. A*, 2005, **109**, 10638–10645.
[48]Z. Rinkevicius and H. Ågren, *Chem. Phys. Lett.*, 2010, **491**, 132–135.
[49]F. Bell, D. Casanova, and M. Head-Gordon, *J. Am. Chem. Soc.*, 2010, **132**, 11314–11322.
[50]C. U. Ibeji and D. Ghosh, *Phys. Chem. Chem. Phys.*, 2015, **17**, 9849–9856.
[51]E. Hossain, S. M. Deng, S. Gozem, A. I. Krylov, X.-B. Wang, and P. G. Wenthold, *J. Am. Chem. Soc.*, 2017, **139**, 11138–11148.
[52]X. Lu, S. Lee, Y. Hong, H. Phan, T. Y. Gopalakrishna, T. S. Herng, T. Tanaka, M. E. Sandoval-Salinas, W. Zeng, J. Ding, D. Casanova, A. Osuka, D. Kim, and J. Wu, *J. Am. Chem. Soc.*, 2017, **139**, 13173–13183.
[53]N. Minezawa and M. S. Gordon, *J. Phys. Chem. A*, 2009, **113**, 12749–12753.
[54]D. Casanova, *J. Chem. Phys.*, 2012, **137**, 084105.
[55]S. Gozem, A. I. Krylov, and M. Olivucci, *J. Chem. Theory Comput.*, 2013, **9**, 284–292.
[56]A. Nikiforov, J. A. Gamez, W. Thiel, M. Huix-Rotllant, and M. Filatov, *J. Chem. Phys.*, 2014, **141**, 124122.
[57]Y. Li, F. Liu, B. Wang, Q. Su, W. Wang, and K. Morukuma, *J. Chem. Phys.*, 2016, **145**, 244311.
[58]Y. Harabuchi, K. Keipert, F. Zahariev, T. Taketsugu, and M. S. Gordon, *J. Phys. Chem. A*, 2014, **118**, 11987–11998.
[59]L. Yue, Y. Liu, and C. Zhu, *Phys. Chem. Chem. Phys.*, 2018, **20**, 24123–24139.
[60]E. Salazar and S. Faraji, *Mol. Phys.*, 2020, **118**, e1764120.
[61]K. D. Nanda and A. I. Krylov, *J. Chem. Phys.*, 2016, **145**, 204116.
[62]K. D. Nanda and A. I. Krylov, *J. Chem. Phys.*, 2017, **146**, 224103.
[63]H. R. Zhekova, M. Seth, and T. Ziegler, *J. Chem. Phys.*, 2011, **135**, 184105.
[64]R. Valero, F. Illas, and D. G. Truhlar, *J. Chem. Theory Comput.*, 2011, **7**, 3523–3531.
[65]N. J. Mayhall and M. Head-Gordon, *J. Chem. Phys.*, 2014, **141**, 134111.
[66]N. J. Mayhall and M. Head-Gordon, *J. Phys. Chem. Lett.*, 2015, **6**, 1982–1988.
[67]N. Orms and A. I. Krylov, *Phys. Chem. Chem. Phys.*, 2018, **20**, 13127–13144.
[68]P. Pokhilko, D. Izmodenov, and A. I. Krylov, *J. Chem. Phys.*, 2020, **152**, 034105.
[69]O. Christiansen, H. Koch, and P. Jørgensen, *Chem. Phys. Lett.*, 1995, **243**, 409–418.
[70]H. J. Monkhorst, *Int. J. Quantum Chem.*, 1977, **12**, 421–432.
[71]E. Dalgaard and H. J. Monkhorst, *Phys. Rev. A*, 1983, **28**, 1217–1222.
[72]H. Koch and P. Jørgensen, *J. Chem. Phys.*, 1990, **93**, 3333–3344.
[73]O. Christiansen, P. Jørgensen, and C. Hättig, *Int. J. Quantum. Chem.*, 1998, **68**, 1–52.
[74]K. Emrich, *Nucl. Phys. A*, 1981, **351**, 379–396.
[75]H. Sekino and R. J. Bartlett, *Int. J. Quantum Chem.*, 1984, **26**, 255–265.
[76]J. F. Stanton and R. J. Bartlett, *J. Chem. Phys.*, 1993, **98**, 7029–7039.
[77]A. I. Krylov, *Annu. Rev. Phys. Chem.*, 2008, **59**, 433–462.
[78]O. Christiansen, H. Koch, P. Jørgensen, and T. Helgaker, *Chem. Phys. Lett.*, 1996, **263**, 530–539.
[79]C. Hättig and F. Weigend, *J. Chem. Phys.*, 2000, **113**, 5154–5161.
[80]C. Hättig and A. Köhn, *J. Chem. Phys.*, 2002, **117**, 6939–6951.
[81]C. Hättig, *J. Chem. Phys.*, 2003, **118**, 7751–7761.
[82]A. Köhn and C. Hättig, *J. Chem. Phys.*, 2003, **119**, 5021–5036.
[83]T. B. Pedersen, A. M. J. Sánchez de Merás, and H. Koch, *J. Chem. Phys.*, 2004, **120**, 8887–8897.
[84]C. Hättig, *Beyond Hartree-Fock: MP2 and Coupled-Cluster Methods for Large Systems*, Vol. 31, John von Neumann Institute for Computing, 2006.
[85]D. Kats, T. Korona, and M. Schütz, *J. Chem. Phys.*, 2006, **125**, 104106.
[86]A. Hellweg, S. A. Grün, and C. Hättig, *Phys. Chem. Chem. Phys.*, 2008, **10**, 4119–4127.
[87]N. O. C. Winter and C. Hättig, *J. Chem. Phys.*, 2011, **134**, 184101.
[88]B. Helmich and C. Hättig, *J. Chem. Phys.*, 2013, **139**, 084114.
[89]A. Köhn and A. Bargholz, *J. Chem. Phys.*, 2019, **151**, 041106.
[90]J. Schirmer, *Phys. Rev. A*, 1982, **26**, 2395–2416.
[91]A. B. Trofimov and J. Schirmer, *J. Phys. B*, 1995, **28**, 2299–2324.
[92]J. Schirmer and A. B. Trofimov, *J. Chem. Phys.*, 2004, **120**, 11449–11464.
[93]A. Dreuw and M. Wormit, *Wiley Interdiscip. Rev.: Comput. Mol. Sci*, 2015, **5**, 82–95.
[94]M. Head-Gordon, R. J. Rico, M. Oumi, and T. J. Lee, *Chem. Phys. Lett.*, 1994, **219**, 21–29.
[95]M. Head-Gordon, M. Oumi, and D. Maurice, *Mol. Phys.*, 1999, **96**, 593–602.
[96]E. Epifanovsky, A. T. B. Gilbert, X. Feng, J. Lee, Y. Mao, N. Mardirossian, P. Pokhilko, A. F. White, M. P. Coons, A. L. Dempwolff, Z. Gan, D. Hait, P. R. Horn, L. D. Jacobson, I. Kaliman, J. Kussmann, A. W. Lange, K. U. Lao, D. S. Levine, J. Liu, S. C. McKenzie, A. F. Morrison, K. D. Nanda,

F. Plasser, D. R. Rehn, M. L. Vidal, Z.-Q. You, Y. Zhu, B. Alam, B. J. Albrecht, A. Aldossary, E. Alguire, J. H. Andersen, V. Athavale, D. Barton, K. Begam, A. Behn, N. Bellonzi, Y. A. Bernard, E. J. Berquist, H. G. A. Burton, A. Carreras, K. Carter-Fenk, R. Chakraborty, A. D. Chien, K. D. Closser, V. Cofer-Shabica, S. Dasgupta, M. de Wergifosse, J. Deng, M. Diedenhofen, H. Do, S. Ehlert, P.-T. Fang, S. Fatehi, Q. Feng, T. Friedhoff, J. Gayvert, Q. Ge, G. Gidofalvi, M. Goldey, J. Gomes, C. E. González-Espinoza, S. Gulania, A. O. Gunina, M. W. D. Hanson-Heine, P. H. P. Harbach, i. A. Hauser, M. F. Herbst, M. Hernández Vera, M. Hodecker, Z. C. Holden, S. Houck, X. Huang, K. Hui, B. C. Huynh, M. Ivanov, A. Jász, H. Ji, H. Jiang, B. Kaduk, S. Kähler, K. Khistyaev, J. Kim, G. Kis, P. Klunzinger, Z. Koczor-Benda, J. H. Koh, D. Kosenkov, L. Koulias, T. Kowalczyk, C. M. Krauter, K. Kue, A. Kunitsa, T. Kus, I. Ladjánszki, A. Landau, K. V. Lawler, D. Lefrancois, S. Lehtola, R. R. Li, Y.-P. Li, J. Liang, M. Liebenthal, H.-H. Lin, Y.-S. Lin, F. Liu, K.-Y. Liu, M. Loipersberger, A. Luenser, A. Manjanath, P. Manohar, E. Mansoor, S. F. Manzer, S.-P. Mao, A. V. Marenich, T. Markovich, S. Mason, S. A. Maurer, P. F. McLaughlin, M. F. S. J. Menger, J.-M. Mewes, S. A. Mewes, P. Morgante, J. W. Mullinax, K. J. Oosterbaan, G. Paran, A. C. Paul, S. K. Paul, F. Pavošević, Z. Pei, S. Prager, E. I. Proynov, A. Rák, E. Ramos-Cordoba, B. Rana, A. E. Rask, A. Rettig, R. M. Richard, F. Rob, E. Rossomme, T. Scheele, M. Scheurer, M. Schneider, N. Sergueev, S. M. Sharada, W. Skomorowski, D. W. Small, C. J. Stein, Y.-C. Su, E. J. Sundstrom, Z. Tao, J. Thirman, G. J. Tornai, T. Tsuchimochi, N. M. Tubman, S. P. Veccham, O. Vydrov, J. Wenzel, J. Witte, A. Yamada, K. Yao, S. Yeganeh, S. R. Yost, A. Zech, I. Y. Zhang, X. Zhang, Y. Zhang, D. Zuev, A. Aspuru-Guzik, A. T. Bell, N. A. Besley, K. B. Bravaya, B. R. Brooks, D. Casanova, J.-D. Chai, S. Coriani, C. J. Cramer, G. Cserey, A. E. DePrince, R. A. DiStasio, A. Dreuw, B. D. Dunietz, T. R. Furlani, W. A. Goddard, S. Hammes-Schiffer, T. Head-Gordon, W. J. Hehre, C.-P. Hsu, T.-C. Jagau, Y. Jung, A. Klamt, J. Kong, D. S. Lambrecht, W. Liang, N. J. Mayhall, C. W. McCurdy, J. B. Neaton, C. Ochsenfeld, J. A. Parkhill, R. Peverati, V. A. Rassolov, Y. Shao, L. V. Slipchenko, T. Stauch, R. P. Steele, J. E. Subotnik, A. J. W. Thom, A. Tkatchenko, D. G. Truhlar, T. Van Voorhis, T. A. Wesolowski, K. B. Whaley, H. L. Woodcock, P. M. Zimmerman, S. Faraji, P. M. W. Gill, M. Head-Gordon, J. M. Herbert, and A. I. Krylov, *J. Chem. Phys.*, 2021, **155**, 084801.

[97] E. Epifanovsky, M. Wormit, T. Kuś, A. Landau, D. Zuev, K. Khistyaev, P. Manohar, I. Kaliman, A. Dreuw, and A. I. Krylov, *J. Comput. Chem.*, 2013, **34**, 2293–2309.

[98] M. Pabst, A. Köhn, J. Gauss, and J. F. Stanton, *Chem. Phys. Lett.*, 2010, **495**, 135–140.

[99] T. H. Dunning, *J. Chem. Phys.*, 1989, **90**, 1007–1023.

[100] D. E. Woon and T. H. Dunning, *J. Chem. Phys.*, 1993, **98**, 1358–1371.

[101] F. Weigend, A. Köhn, and C. Hättig, *J. Chem. Phys.*, 2002, **116**, 3175–3183.

[102] A. Dutta and C. D. Sherrill, *J. Chem. Phys.*, 2003, **118**, 1610–1619.

[103] S. Das, D. Mukherjee, and M. Kállay, *J. Chem. Phys.*, 2010, **132**, 074103.

[104] C. Li and F. A. Evangelista, *J. Chem. Theory Comput.*, 2015, **11**, 2097–2108.

[105] P. G. Wenthold, R. R. Squires, and W. C. Lineberger, *J. Am. Chem. Soc.*, 1998, **120**, 5279–5290.

[106] M. Winkler and W. Sander, *J. Aust. Chem.*, 2010, **63**, 1013–1047.

[107] B. N. Figgis and R. L. Martin, *J. Chem. Soc.*, 1956, pp. 3837–3846.

[108] C. López, R. Costa, F. Illas, C. de Graaf, M. M. Turnbull, C. P. Landee, E. Espinosa, I. Mata, and E. Molins, *Dalton Trans.*, 2005, pp. 2322–2330.

[109] M. R. Pederson and T. Baruah, *Molecular Magnets: Phenomenology and Theory. In: Handbook of Magnetism and Magnetic Materials*, John Wiley & Sons, 2007.

[110] J.-P. Malrieu, R. Caballol, C. J. Calzado, C. de Graaf, and N. Guihéry, *Chem. Rev.*, 2013, **114**, 429–492.